Acta Cryst. (1979). A35, 925–933

An Empirical Method for Correcting Rotation-Camera Data for Absorption and Decay Effects

BY DAVID STUART AND NIGEL WALKER

Department of Biochemistry, University of Bristol, Bristol BS8 1TD, England

(*Received* 27 *March* 1979; *accepted* 11 *June* 1979)

Abstract

When the same set of structure factors is measured twice from separate crystals, some of the differences between the two sets of data will be due to differences in absorption and crystal disorder. This will particularly affect the isomorphous-replacement method. By carefully choosing crystals of the same shape and size, and by recording the reflections in the same order, these sources of error may sometimes be minimized. However, there will be cases where serious errors of this kind will prove unavoidable. A method of deriving a correction for the absorption and decay differences between two sets of structure factors after the measurements have been made is presented. The method is designed to correct protein data collected on a rotation camera. Where an absorption-corrected subset of the observed data is available, the rotation-camera data may be corrected to this. Where this cannot be done, the method allows a relative correction between native and isomorphous-derivative data sets. The method has been implemented on a mini-computer. Results are presented which show that in some cases a substantial improvement in the quality of the data is obtained, as judged by the agreement of symmetry-related amplitudes. Furthermore, the method is capable of improving the reliability of measurements of anomalous scattering from heavy-atom-substituted isomorphous derivatives. The potential usefulness of this method is discussed.

1. Introduction

In recent years the rotation camera has been used increasingly for the X-ray determination of protein structures. In many of these investigations absorption effects are likely to be the most serious source of systematic errors; however, in most cases no attempt to correct for absorption has been made.

The usefulness of absorption corrections for the improvement of protein data has been demonstrated by both North, Phillips & Mathews (1968) and Kopfmann & Huber (1968). Both methods are empirical and have so far been mainly used for the correction of diffractometer data. Recently an experimental method for the rotation camera has become available with the marketing of a device by Enraf–Nonius. A similar approach (Schwager, Bartels & Huber, 1973) has been used in the successful structure detèrmination of trypsinogen (Bode, Fehlhammer & Huber, 1976). The method relies upon measuring the relative attenuation of the direct X-ray beam for different positions of the crystal and is therefore only valid where the beam is both monochromatic and contained entirely within the crystal; and of course data already collected cannot be treated. Two methods have been suggested for the correction of extant data. The analytical method (Busing & Levy, 1957) is not suitable for proteins since the computing time required would be enormous and the mother liquor around the crystal prevents the accurate determination of the absorption suffered by the incident and diffracted beams. Katayama, Sakabe & Sakabe (1972) recognized that, due to the smoothly varying nature of absorption effects, a good approximation to the transmission is a Fourier series in the polar angles of both the incident and diffracted beams, where only the low-order terms are important. The values for these coefficients are obtained by the analysis of symmetry-related reflections within a single data set. This requires high lattice symmetry and also that equivalent reflections do not have the same absorption factors, conditions which are often not fulfilled.

We have developed a method to correct extant structure factor amplitudes from protein crystals collected on the rotation camera. If a set of structure factors has been measured twice (*i.e.* from two different crystals) then the differences will in part be due to differing absorption and decay effects. Commonly in the course of a protein structure determination, a low-resolution absorption-corrected data set is obtained before high-resolution studies are begun. We have used this low-resoluton data set as a reference set to obtain absorption factors for the high-resolution data by a least-squares fitting process. We have also estimated a relative correction between the native protein and

0567-7394/79/060925-09$01.00

isomorphous heavy-atom derivative data to improve the measurement of isomorphous differences and anomalous scattering. The method uses some aspects of the approach of Katayama *et al.* (1972) and may also be related to the methods of North *et al.* (1968) and Kopfmann & Huber (1968).

2. The method

2.1. *Absorption correction*

Let the two sets of structure factors be designated $F_j^{(1)}$ and $F_j^{(2)}$; we modify the observed values of $F_j^{(1)}$ by the following empirical correction:

$$F_{j\,\mathrm{mod}}^{(1)} = F_j^{(1)} \left\{ h_i + \sum_n \sum_m [P_{n,m} \sin(n\varphi_s + m\mu_s) + Q_{n,m} \cos(n\varphi_s + m\mu_s)] \right\}, \tag{2.1}$$

where h_i is a scale factor for film pack i, $F_{j\,\mathrm{mod}}^{(1)}$ is the modified value of the structure factor amplitude $F_j^{(1)}$, φ_s and μ_s are angles defining the diffracted beam, and $P_{n,m}$ and $Q_{n,m}$ are Fourier coefficients.

Note that this expression models the absorption as a trigonometric series in the polar angles φ_s and μ_s of the scattered beam (Fig. 1). If the form of this expression is a good model for the effects of absorption then the choice of suitable values for h_i, $P_{n,m}$ and $Q_{n,m}$ should produce a set of structure factor amplitudes, $F_{j\,\mathrm{mod}}^{(1)}$ which agree better with $F_j^{(2)}$ (which was indeed found to be the case in practice). Values for the coefficients h_i, $P_{n,m}$ and $Q_{n,m}$ are obtained by minimizing the sum of the squares of the residuals, R_j:

$$\sum_j (R_j)^2, \tag{2.2}$$

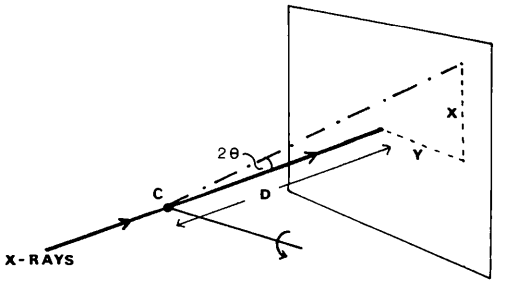

Fig. 1. Relationship between the diffraction geometry and film coordinate system. C is the crystal position, D is the crystal-to-film distance. If φ_p is the camera spindle angle (see Fig. 5) then φ_s = arctan $(-X/D)$ + φ_p and μ_s = arctan (Y/D). The scattering angle, 2θ = arctan $[(X^2 + Y^2)^{1/2}/D]$. The direction of rotation about the spindle axis is shown.

where

$$R_j = \left(F_j^{(2)} - F_j^{(1)} \left\{ h_i + \sum_n \sum_m [P_{n,m} \sin(n\varphi_s + m\mu_s) + Q_{n,m} \cos(n\varphi_s + m\mu_s)] \right\} \right) \omega_j, \tag{2.3}$$

and ω_j is a suitable weighting factor.

The form of the approximation used here may be compared with previous approximate solutions of the absorption problem.

The transmission factor for any diffracted beam is

$$T_{\mathrm{p,s}} = \frac{1}{v} \int_v \exp[-M(x_\mathrm{p} + x_\mathrm{s})]\, \mathrm{d}v, \tag{2.4}$$

where M is the mass absorption coefficient for the crystal and x_p and x_s are the primary and secondary beam path lengths. To make this expression tractable, two approximations have been used with success. We can apply the Fourier series expansion to both of these approximations and compare the results with our expression (2.1). The analysis is carried out for both approximations in parallel below; (*a*) refers to North, Phillips & Mathews (1968), and (*b*) to Kopfmann & Huber (1968) (note that the symbols will have different values in the two approximations).

$$T_{\mathrm{p,s}} = (T_\mathrm{p} + T_\mathrm{s})/2 \tag{2.5a}$$

$$T_{\mathrm{p,s}} = T_\mathrm{p} . T_\mathrm{s}. \tag{2.5b}$$

Since the movement of the crystal during the exposure of any rotation photograph is small, the primary-beam transmission may be taken as a constant, k_i, for each photograph i. Expressions (2.5*a* and *b*) then become:

$$T_{\mathrm{p,s}} = (k_i + T_\mathrm{s})/2 \tag{2.6a}$$

$$T_{\mathrm{p,s}} = k_i T_\mathrm{s}. \tag{2.6b}$$

Now, following the arguments of Katayama *et al.* (1972), we represent the secondary-beam transmission as a Fourier series in the polar angles φ_s and μ_s. These are defined in Fig. 1. Thus:

$$T_{\mathrm{p,s}} = \left\{ k_i + \sum_n \sum_m [P_{n,m} \sin(n\varphi_s + m\mu_s) + Q_{n,m} \cos(n\varphi_s + m\mu_s)] \right\}/2 \tag{2.7a}$$

$$T_{\mathrm{p,s}} = k_i \sum_n \sum_m [P_{n,m} \sin(n\varphi_s + m\mu_s) + Q_{n,m} \cos(n\varphi_s + m\mu_s)]. \tag{2.7b}$$

These expressions are true for any one film, but of course the transmission of any beam is dependent only on the angles φ and μ and not on film number. There

will inevitably be differences in scale between films, due in part to different photographic-development conditions. If this scale factor, g_l, is applied to (2.7*a* and *b*) then the equations are valid for the complete data set:

$$T_{p,s} = \Big\{ g_l k_l + g_l \sum_n \sum_m [P_{n,m} \sin(n\varphi_s + m\mu_s) + Q_{n,m} \cos(n\varphi_s + m\mu_s)] \Big\}/2 \qquad (2.8a)$$

$$T_{p,s} = g_l k_l \sum_n \sum_m [P_{n,m} \sin(n\varphi_s + m\mu_s) + Q_{n,m} \cos(n\varphi_s + m\mu_s)]. \qquad (2.8b)$$

The zero-order terms may be taken out of the summations to give

$$T_{p,s} = \Big\{ g_l k_i + g_l Q_{0,0} + g_i \sum_n \sum_m [P_{n,m} \sin(n\varphi_s + m\mu_s) + Q_{n,m} \cos(n\varphi_s + m\mu_s)] \Big\}/2 \qquad (2.9a)$$

$$T_{p,s} = g_l k_l Q_{0,0} + g_l k_i \sum_n \sum_m [P_{n,m} \sin(n\varphi_s + m\mu_s) + Q_{n,m} \cos(n\varphi_s + m\mu_s)]. \qquad (2.9b)$$

Grouping some of the unknowns $Q_{0,0}, g_l, k_l$:

$$T_{p,s} = \Big\{ U_l + g_l \sum_n \sum_m [P_{n,m} \sin(n\varphi_s + m\mu_s) + Q_{n,m} \cos(n\varphi_s + m\mu_s)] \Big\}/2 \qquad (2.10a)$$

$$T_{p,s} = U_l + g_i k_l \sum_n \sum_m [P_{n,m} \sin(n\varphi_s + m\mu_s) + Q_{n,m} \cos(n\varphi_s + m\mu_s)]. \qquad (2.10b)$$

Neither of these expressions is easily solved and instead we use equation (2.1) which is conveniently linear in all the unknowns.

Note that equation (2.1) represents a modifying function for scattered amplitudes whereas (2.10*a* and *b*) operate upon scattered intensities. We have found by experimentation that for the effects observed in our test case (see §3 below) the use of amplitudes gives some advantages. The relationship between the two is very simple: a transmission factor on amplitude is the square root of a transmission factor applied to intensities, and we found that this permitted a better modelling of the effect. In particular at the extremes of the observed range of φ_s the transmission surface obtained on the basis of intensities was rather poorly defined. This may in part be due to the lower weight given to the (relatively weaker) data observed at high scattering angles and also to the more rapid variation of transmitted intensity with respect to the polar angles φ and μ. Throughout the subsequent discussion all modifications and improvements will be discussed in terms of structure factor amplitude; hence 'transmitted amplitude' will be used as analogous to transmission. When comparing expression (2.1) with (2.10*a* and *b*) it should be borne in mind that the former represents absorption while the latter are transmission factors. Expressions (2.1) and (2.10*a* and *b*) are obviously related; the simplification achieved in (2.1) comes from only allowing film number dependency in the zero-order term of the Fourier series. Thus the process fits a curve of the same shape to all the films but allows it to 'slide' up or down (with respect to amplitude transmission). This is illustrated in Fig. 2.

If it is assumed that the scale factors between the films are similar, then equation (2.1) should approximate equation (2.10*a*) well. However, it will only approach equation (2.10*b*) when, in addition, the incident-beam transmission is fairly constant for all the data.

2.2. *Decay correction*

In the case of proteins, it is common for different crystals to exhibit different degrees of order. If this occurs there will be a systematic difference between the data sets with respect to the scattering angle, 2θ. For any film, 2θ is related simply to φ_s and μ_s; thus a difference in order between $F_j^{(1)}$ and the scaling data $F_j^{(2)}$ will be indistinguishable from an absorption effect. However, the relationship between 2θ and φ_s is different for each film since φ_s is dependent on φ_p (see Fig. 1) as well as the position on the film, thus invalidating the assumption necessary to arrive at equations (2.8*a* and *b*). This effect is shown schematically in Fig. 3.

Furthermore, crystal decay may be manifest as a change in crystal order with time. In addition to invalidating some of the assumptions of our absorption-correction method, this may in itself be a serious

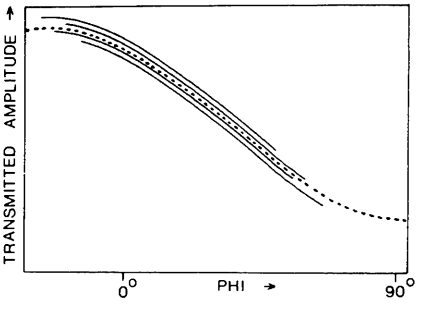

Fig. 2. Diagrammatic representation of the transmitted amplitude surfaces of different films from the same crystal. The dotted line shows the $\mu_s = 0$ section through a hypothetical absorption surface. Since the structure factor amplitudes for the different films will not be on precisely the same scale, the apparent transmission at any point will be affected by a scale factor, g_i, for that film, i. The $\mu_s = 0$ sections through these apparent absorption surfaces are shown as solid lines.

source of systematic error. In order to correct for both differences in crystal order and decay we modify the data by the following expression:

$$F^{(1)}_{j\text{temp}} = f_i F^{(1)}_{j\text{mod}} \exp[l_1 s + l_2(i+10)s + l_3(i+10)^2 s \ldots], \quad (2.11)$$

where $s = \sin^2\theta/\lambda^2$, f_i is a scale factor for film i, and l_1, l_2, l_3 ... are temperature-factor coefficients. This represents the crystal decay as a scale factor and temperature factor related to film number. The value of 10 added to the film number provides a better model of this decay. Very few terms of the polynomial should be needed for a good correction. Taking logs of equation (2.11) gives:

$$\log F^{(1)}_{j\text{temp}} = \log f_i + \log F^{(1)}_{j\text{mod}} + l_1 s + l_2(i+10)s + l_3(i+10)^2 s \ldots. \quad (2.12)$$

If we suppose that differences between $F^{(1)}_j$ and $F^{(2)}_j$ due to absorption have been eliminated, then remaining differences due to crystal-decay effects should be reduced by minimizing the sum $\sum_j (R_{ij})^2$, where

$$R_{ij} = \{\log F^{(2)}_j - [\log f_i + \log F^{(1)}_{j\text{mod}} + l_1 s + l_2(i+10)s + l_3(i+10)^2 s \ldots]\}\omega_{ij}; \quad (2.13)$$

ω_{ij} is a suitable weighting factor. The unknowns, $\log f_i$, l_1, l_2, l_3 ..., may be evaluated by the usual procedure of least squares since the observational equations are linear with respect to all of them.

The effects are not strictly separable. In order to apply equation (2.1) we have to assume that decay effects have been corrected, and in order to apply equation (2.11) we have to assume that absorption effects have been corrected. Alternate cycles of absorption and decay correction are performed always using the values from the previous cycle of least squares to calculate the new coefficients. The process has been found to converge satisfactorily (§ 3.1).

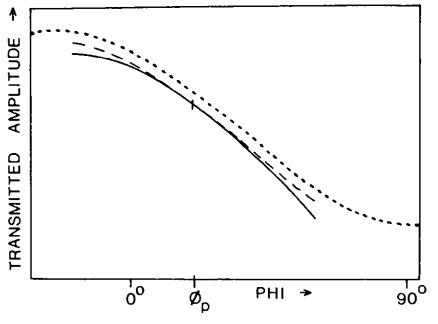

Fig. 3. The $\mu_s = 0$ section of a hypothetical transmitted amplitude surface is shown dotted. The dashed and solid lines show the apparent surface for a film i. The dashed line shows the effect of a scale factor only, g_i, and the full line the deviation from this introduced when $F^{(1)}_j$ is less ordered than $F^{(2)}_j$.

2.3. *Implementation*

Two computer programs have been written: *ABSOLV* estimates the absorption and decay correction coefficients and writes the results to a file which may be used by *ABSPLY* to correct the data. The programs have been designed to form part of the system for processing rotation-camera data used at Bristol University, and run under DOS on a PDP 11/45 mini-computer with 28K words of storage and two 1·2 M word magnetic discs. The programs are written almost entirely in Fortran IV with a few very short assembler language subroutines. The correction is evaluated and applied after Lorentz–polarization correction and scaling of the different films within each pack, but before averaging symmetry repeats.

Initially the data are brought to approximately the same scale on the basis of reflections common to at least two data sets. This is achieved by the simplification of the method of Fox & Holmes (1966) described by Ford & Rollett (1968).

The program then performs alternate cycles of estimation of absorption-correction and decay-correction parameters, always using the values from the previous cycle of least squares to calculate the new coefficients.

Contributions to the normal equations are included from all reflections in the data to be corrected which are recorded fully on one film and whose indices, when reduced to a unique set, correspond to those of a reflection in the scaling set. For this purpose any differences between Friedel mates are ignored.

The weighting functions, ω_j and ω_{ij}, chosen were $1/\sigma_j$ for the absorption correction and $F^{(1)}_j/\sigma_j$ for the decay correction.

The value of σ_j for each reflection is derived from the counting-statistics standard deviation in intensity (σ^I_j) defined by Stuart, Levine, Muirhead & Stammers (1979):

$$\sigma_j = \sigma^I_j / F^{(1)}_j. \quad (2.14)$$

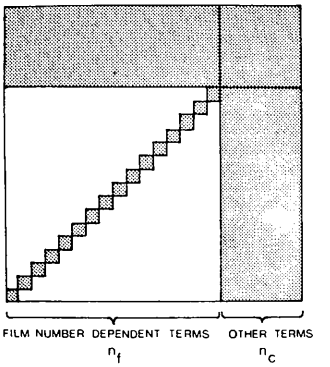

Fig. 4. Schema of the normal equations. Only the shaded areas are evaluated.

The normal equations for both the absorption and decay corrections are of order n_f plus n_c, where n_f is the number of films and n_c is the number of absorption or decay coefficients. However, not all of the $(n_f + n_c)^2$ terms need be set up since there is no correlation between the different scale factors and many off-diagonal terms are zero. This is illustrated by the shaded area in Fig. 4. The matrix is solved by Gauss–Jordan elimination.

The Fourier series in equation (2.1) was constructed from the minimum number of terms commensurate with a good model [as judged by the r.m.s. values of the residual R_j in equation (2.3)].

After each cycle of absorption correction, a φ curve is printed using the latest parameters, and there is the option of printing a map of transmitted amplitude for any given film with respect to φ_s and μ_s. Following a cycle of decay-correction calculation, the factor to be applied is printed for each film.

3. A test of the method

The method was developed and tested on yeast phosphoglycerate kinase crystals for which previously collected 2·5 Å resolution rotation-camera data were available (Shaw, Bryant, Walker, Watson & Wendell, 1979). This enzyme crystallizes in the space group $C2$ with unit-cell dimensions $a = 126{\cdot}6$, $b = 54{\cdot}4$, $c = 93{\cdot}0$ Å and $\beta = 133{\cdot}9°$. In order to obtain accurate measures of the anomalous-dispersion effects, the crystals were mounted as shown in Fig. 5. From Figs. 1 and 5 it can be seen that for the diffracted beams hkl and $h\bar{k}l$ (which constitute a Bijvoet pair):

$$\varphi_p\, hkl = \varphi_p\, h\bar{k}l \tag{3.1}$$

$$\varphi_s\, hkl = \varphi_s\, h\bar{k}l \tag{3.2}$$

$$\mu_s\, hkl = -\mu_s\, h\bar{k}l. \tag{3.3}$$

This mounting would be expected to result in very large differences in absorption on rotation about φ since previous experiments using the method of North *et al.* (1968) on a diffractometer had shown that changes in intensity of up to 50% occurred for a more favourable mounting (rotation about **a***). The data were well suited to the method described; the rotation range per photograph was reasonably small (3°); thus the incident-beam absorption varied little within one film, while sufficient films were obtained per crystal (usually 20) to enable a wide φ range to be sampled by each crystal.

Table 1 lists the data sets used in this study and gives some details of the application of our method. Some 30% of the rotation-camera data had a reflecting range spanning two photographs. These partially recorded reflections were not used in deriving the correction, but were modified when the correction was applied using the program *ABSPLY*. Unless otherwise stated, the analyses of the data presented below include these reflections. Firstly, native crystals 5 and 3 were corrected against the diffractometer data *D*7. The crystallographically equivalent reflections were then averaged to give the unique set of reflections for that crystal, which were used to correct the derivative data (crystals 7 and 6 respectively).

For the correction of native rotation-camera data, only a φ correction was calculated and applied. This was because the maximum μ angle common to the two data sets was limited to the scattering angle of the low-resolution diffractometer data, whereas in φ the common reflections spanned the full rotation range of the crystal. The coefficients used were [see equation (2.1)] $P_{n,m}$ and $Q_{n,m}$, where $n = 2, 3, 4$ and $m = 0$. Native data corrected in this way were then used to correct isomorphous-derivative rotation data in both φ and μ. The coefficients used here were $P_{n,m}$ and $Q_{n,m}$ for the following pairs of n and m: 2,0; 3,0; 4,0; 0,1; 0,2; 1,1; 2,2. We have found that for the decay correction, the series in l converged rapidly and use of the first three terms was adequate.

3.1. *Convergence*

We judge the convergence of the iteration procedure by the stabilization of the values obtained for the absorption and decay corrections. This is illustrated in Fig. 6. The correction uses those 3536 of the 18787 reflections of crystal 5 which correspond to data in *D*7 (see Table 1). The absorption correction is in φ only. The initial cycle is one of estimation of absorption-correction parameters. It can be seen that the process converges quite rapidly and in this case we halted after the eighth estimation of absorption coefficients, by which stage the program had been running for about 2 h; eight cycles were also used for correcting crystal 3 whilst the correction in φ and μ for crystals 7 and 6 (see Table 1) required 15 cycles and about 10 h.

In order to establish whether the systematic errors of absorption and θ-dependent decay were separable by our method, an artificial (film-number-dependent) temperature factor was applied to the data from crystal

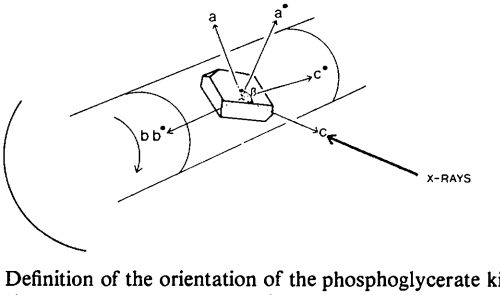

Fig. 5. Definition of the orientation of the phosphoglycerate kinase crystals as mounted on the rotation camera with $\varphi_p = 0$. The direction of rotation about the spindle axis is shown.

Table 1. *Data used to test the method*

The derivative diffractometer sets *D*1 to *D*6 were collected as described by Bryant, Watson & Wendell (1974). The first set contains the 10% most-intense reflections to a resolution of 3·5 Å, the second contains the next strongest tenth, and so on. The six corresponding native data sets were merged together with additional 5 Å data to produce *D*7. φ_p is defined in Fig. 5.

Data set	Source of data	Type	Minimum spacing (Å)	Total number of reflections: unique in parentheses	Number of reflections used in deriving correction: unique in parentheses	φ_p range (°)	Number of films	Type of absorption correction applied
Crystal 5	Rotation camera	Native	2·5	18787 (7245)	3526 (1520)	0–60	20	*ABSOLV* using *D*7 (φ alone)
Crystal 3	Rotation camera	Native	2·5	17734 (6757)	3607 (1629)	54–111	19	*ABSOLV* using *D*7 (φ alone)
Crystal 7	Rotation camera	Hg derivative	2·5	17904 (6801)	12043 (6104)	0–60	20	*ABSOLV* using corrected crystal 5 unique reflections (φ and μ)
Crystal 6	Rotation camera	Hg derivative	2·5	18931 (7173)	11963 (5989)	54–114	20	*ABSOLV* using corrected crystal 3 unique reflections (φ and μ)
*D*1 to *D*6	Diffractometer	Hg derivative	3·5	(3749)				North *et al.* (1968)
*D*7	Diffractometer	Native data sets merged	3·5	(3831)				North *et al.* (1968)

5. A fivefold perturbation was applied to the argument of the exponent in equation (2.11) (this was achieved by setting f_i to 1, l_2 to -1 and all other coefficients to zero). After 10 cycles of absorption and decay correction the program had modelled this perturbation to an average accuracy of 1·5%.

3.2. *Absorption-correction results*

Fig. 7 shows the normalized transmitted amplitude curves in φ obtained for the four crystals. Note that the general features of these curves are consistent with those expected from the crystal morphology.

The normalized transmitted amplitude surfaces in φ_s and μ_s for two films of crystal 7 are shown in Fig. 8(*a*, *b*) and for two films of crystal 6 in Fig. 8 (*c*, *d*). These contour maps show that there is a significant increase in relative absorption with increasing μ_s. For crystal 6 the transmitted amplitude of the secondary beam for plus and minus μ_s is nearly the same; thus the absorption suffered by the Bijvoet pairs, *hkl* and $h\bar{k}l$,

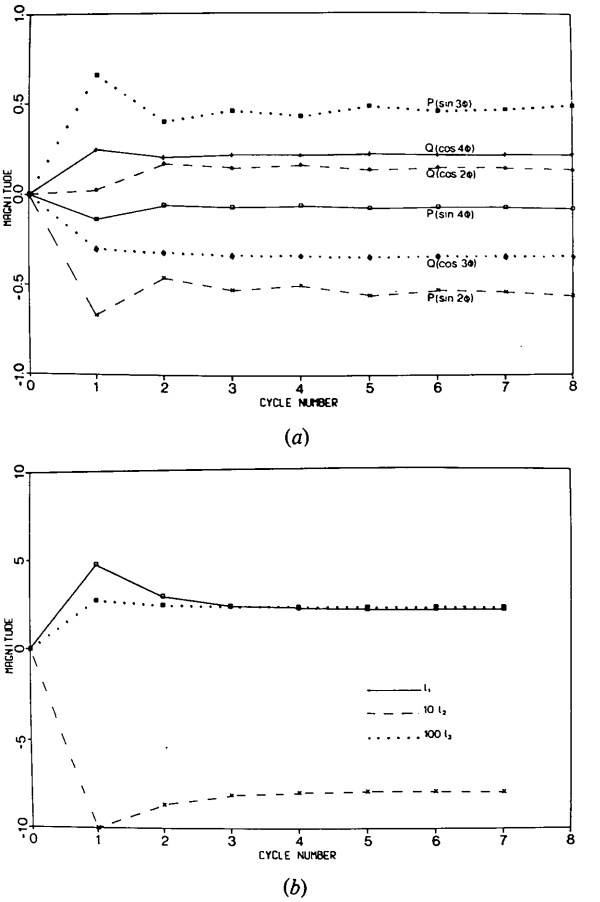

Fig. 6. Convergence of the absorption and decay modelling for crystal 5. The values calculated for each coefficient at every cycle are shown. (*a*) The values for the absorption coefficients, see equation (2.1). (*b*) The values for the decay coefficients as defined in equation (2.11).

will be similar. However, the asymmetry of the transmitted amplitude with respect to plus and minus μ_s is quite marked for crystal 7 and this would prevent accurate measurement of the anomalous differences in the absence of a correction.

3.3. *Decay-correction results*

Fig. 9 shows the film-number-dependent temperature-factor curves obtained for the four crystals. While crystals 5 and 7 have a similar crystal order, it can be seen that crystal 6 is more ordered than crystal 3. All four crystals tend to become less ordered towards the end of data collection.

3.4. *Analysis of results*

The relative discrepancies between each of the four crystals corrected and their corresponding scaling sets were evaluated both before and after correction. The results are given in Table 2.

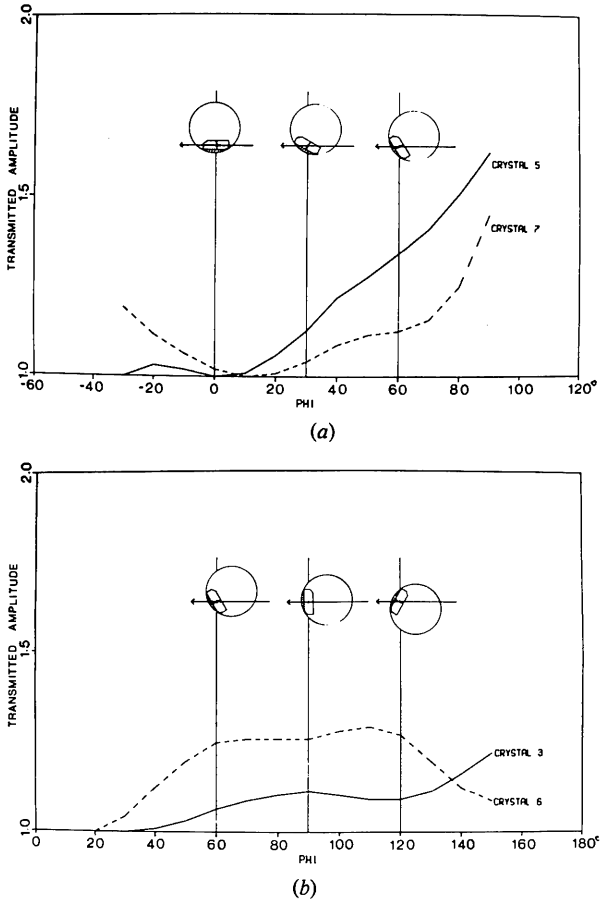

Fig. 7. Plots of the normalized transmitted amplitude (for $\mu_s = 0$) with increasing φ, in degrees. The solid lines correspond to native crystals, and the derivative crystals are shown dashed. The orientation of the crystal at φ_p values of 0, 30, 60, 90 and 120° is shown. The arrow indicates the direction of the X-ray beam. (*a*) Crystals 5 and 7. (*b*) Crystals 3 and 6.

We have analysed the agreement of symmetry-related reflections measured from the same crystal in terms of R', defined as

$$R' = \frac{\sum_{\mathbf{h}} \sum_{j=1}^{n} \left| |\bar{F}_{\mathbf{h}}| - |F_{\mathbf{h}_j}| \right|}{\sum_{\mathbf{h}} {}_n|\bar{F}_{\mathbf{h}}|}. \tag{3.4}$$

For the heavy-atom-derivative crystals this measure includes real differences due to anomalous dispersion. It can be seen from Table 3 that application of the absorption/decay correction improves the internal consistency of measurements from each crystal as judged by this measure. From Fig. 7 it can be seen that crystals 5 and 7 suffered greater absorption effects than crystals 3 and 6 and this is reflected in the more striking improvement in the R' factors for crystals 5 and 7. This improvement is investigated further in Figs. 10 and 11 which show the internal agreement, as defined above, analysed with respect to film number and resolution respectively. It can be seen that a substantial improvement in the quality of the data has been obtained over the full range of resolution.

Table 4 shows a more detailed analysis of the heavy-atom-derivative data measured on the rotation camera. The overall R factor is in this case

$$R = \frac{\sum_{\mathbf{h}} \left| |F_{\mathbf{h}_i}| - |F_{\mathbf{h}_j}| \right|}{\sum |\bar{F}_{\mathbf{h}}|}, \tag{3.5}$$

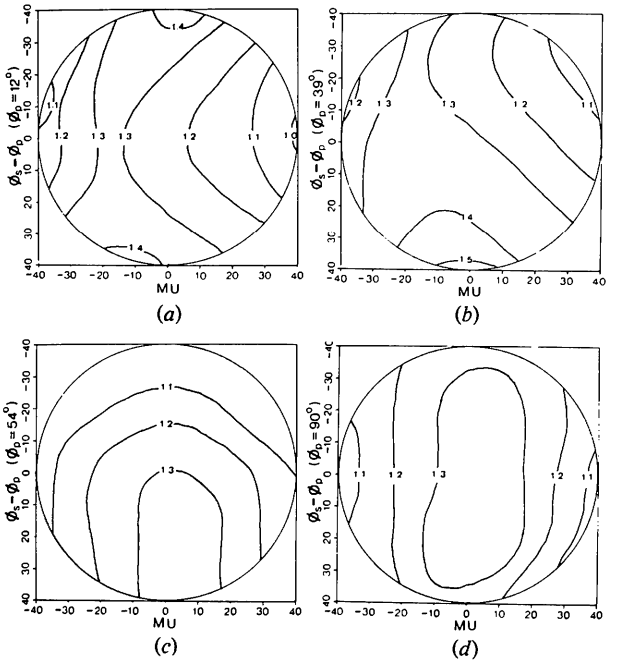

Fig. 8. Normalized transmitted amplitude surfaces for selected films of the two derivative crystals. (*a*) Crystal 7: film 5. (*b*) Crystal 7: film 14. (*c*) Crystal 6: film 1. (*d*) Crystal 6: film 13. The axes are marked in degrees.

and is a measure of the agreement of reflections common to data sets i and j. The corrected data from crystals 7 and 6 agree similarly with the diffractometer data, but this has been achieved by a much greater improvement in the data for crystal 7 as compared to crystal 6. Furthermore, the corrected rotation-camera data sets are in excellent agreement with each other.

The anomalous difference Patterson map for crystal 7 after correction (Fig. 12*b*) shows a dramatic increase in the height of the Hg peak at the expected position of this single-site derivative, compared to the anomalous difference Patterson map for the uncorrected data (Fig. 12*a*). With the height of the origin peak set to 200, the uncorrected data gives a peak height of 7 compared to 14 after correction. However, there appears to be a slight increase in the noise level after correction. Similar calculations with crystal 6 showed very little difference in Hg peak height, or noise level, between the anomalous difference Patterson maps before and after correction, as was expected from the more symmetrical nature of the transmitted amplitude surfaces (see Fig. 8*c* and *d*).

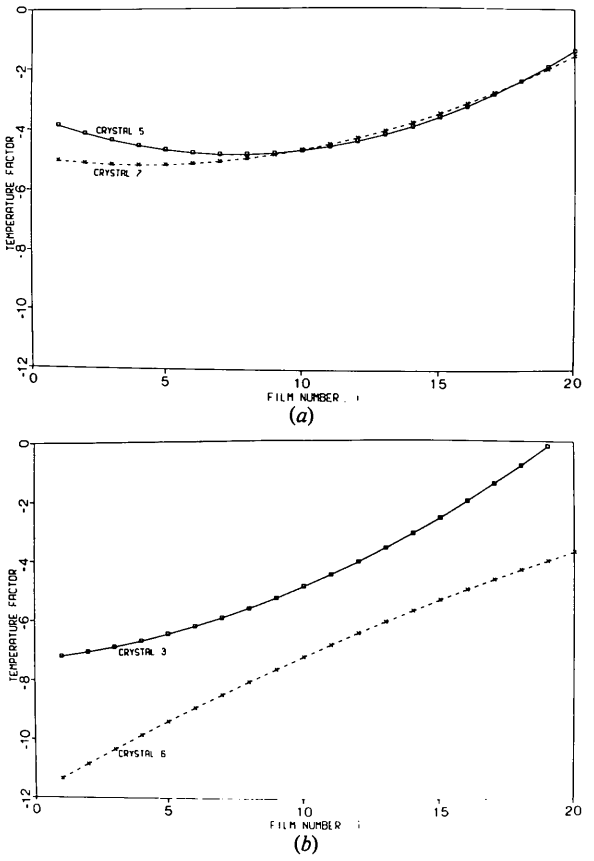

Fig. 9. Plots of the 'temperature factor' $[l_1 + l_2(i + 10) + l_3(i + 10)^2]$ with respect to film number, i. (*a*) Crystals 5 and 7. (*b*) Crystals 3 and 6.

Table 2. *Relative residuals before and after correction*

Column (1) indicates the data sets to be corrected. Column (2) shows the average deviation of $F_j^{(1)}$ from $F_j^{(2)}$ as a percentage of the magnitude of $F_j^{(2)}$. Column (3) shows the value of this average relative deviation after correction for absorption and decay.

(1) Data set	(2) Relative residual before correction (%)	(3) Relative residual after correction (%)
Crystal 5	9·43	6·13
Crystal 3	7·78	6·96
Crystal 7	16·69	14·39
Crystal 6	18·09	16·32

4. Discussion

We feel from the evidence shown above that the application of this method produced a substantial improvement in the quality of the data. It is difficult at this stage to say how useful the method will prove for other cases, especially since the availability of a medium-resolution absorption-corrected data set and a large rotation range per crystal is likely to prove the exception rather than the rule. The method may prove useful in two rather different ways. Firstly, if some absorption-corrected data are available covering a sufficient part of the φ range sampled by the rotation-camera data to constrain the Fourier coefficients, then an absorption correction may be made as indicated above. The 'correct' data may of course come from any source: rotation camera, precession camera, diffractometer, or even in the final stages of a structure refinement from a structure factor calculation. If, however, no corrected data can be obtained, the method can be used to correct between different data sets collected on the rotation camera. Such a correction is likely to prove useful in improving the measurement of isomorphous and anomalous differences. Whichever way the method

Table 3. *Agreement of crystallographically equivalent reflections measured on different photographs collected from the same crystal*

		R' factor (%)			
		Crystal 5	Crystal 3	Crystal 7	Crystal 6
Only fully recorded reflections	Before correction	3·9	3·8	5·1	5·3
	After correction	2·8	3·5	3·7	5·3
Fully recorded and partial reflections	Before correction	4·0	4·0	5·2	5·2
	After correction	2·9	3·5	3·7	4·9

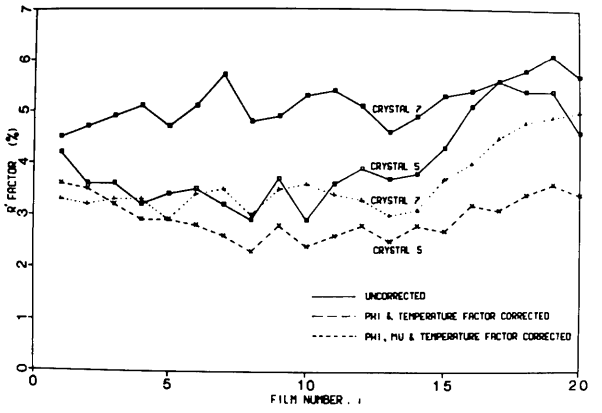

Fig. 10. Agreement of reflections on film i with equivalent reflections from all other films. The measure R' is defined in the text.

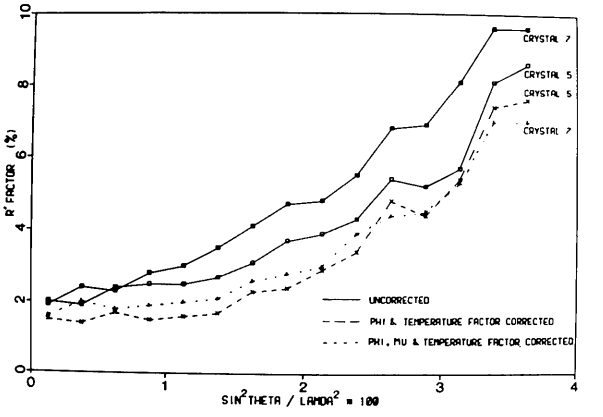

Fig. 11. Agreement of symmetry-related reflections with respect to resolution. R' is defined in the text.

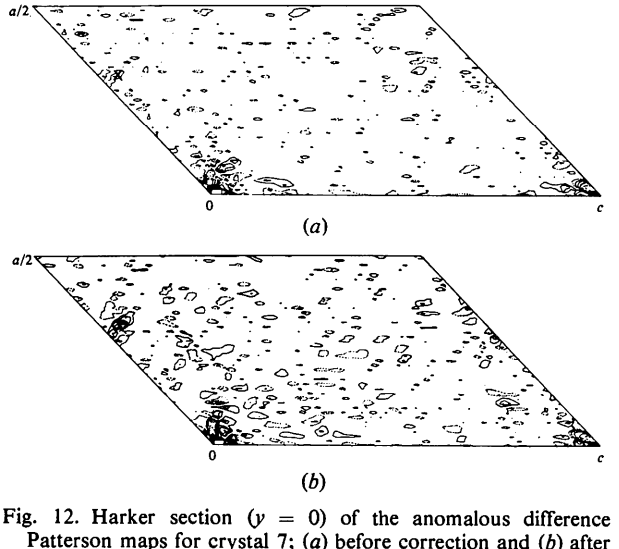

Fig. 12. Harker section (y = 0) of the anomalous difference Patterson maps for crystal 7; (*a*) before correction and (*b*) after correction. $(F_{hkl} - F_{h\bar{k}l})^2$ were the terms used for the summation. The origin peak was set to 200 and the contours drawn at intervals of 3. The zero contour was omitted. × marks the expected position of the Hg peak.

Table 4. *Agreement of reflections common to both the rotation camera and diffractometer Hg derivative data sets; before and after correction*

Data sets		*R* factor before correction (%)	*R* factor after correction (%)
*D*1	with Crystal 6	7·2	5·8
*D*2		7·0	5·4
*D*3		8·2	6·6
*D*4		8·0	6·6
*D*5		8·3	7·2
*D*6		8·2	7·3
*D*1	with Crystal 7	10·3	5·4
*D*2		9·0	6·2
*D*3		9·4	7·1
*D*4		8·6	6·2
*D*5		8·9	6·3
*D*6		10·5	8·0
Crystal 6 with Crystal 7		4·6	2·6

is applied, some experimentation will probably be required to determine which coefficients should be used in equation (2.1).

We are indebted to Mike Levine and the late Peter Wendell for many useful discussions, and to Peter Shaw for providing the rotation-camera data. We are grateful for financial support from the SRC during the course of this work, and also for the excellent computing facilities provided under the auspices of Dr H. C. Watson.

References

BODE, W., FEHLHAMMER, H. & HUBER, R. (1976). *J. Mol. Biol.* **106**, 325–335.

BRYANT, T. N., WATSON, H. C. & WENDELL, P. L. (1974). *Nature (London)*, **247**, 14–17.

BUSING, W. R. & LEVY, H. A. (1957). *Acta Cryst.* **10**, 180–182.

FORD, G. C. & ROLLETT, J. S. (1968). *Acta Cryst.* B**24**, 293–294.

FOX, G. C. & HOLMES, K. C. (1966). *Acta Cryst.* **20**, 886–891.

KATAYAMA, C., SAKABE, N. & SAKABE, K. (1972). *Acta Cryst.* A**28**, 293–295.

KOPFMANN, G. & HUBER, R. (1968). *Acta Cryst.* A**24**, 348–351.

NORTH, A. C. T., PHILLIPS, D. C. & MATHEWS, F. S. (1968). *Acta Cryst.* A**24**, 351–359.

SCHWAGER, P., BARTELS, K. & HUBER, R. (1973). *Acta Cryst.* A**29**, 291–295.

SHAW, P. J., BRYANT, T. N., WALKER, N. P. C., WATSON, H. C. & WENDELL, P. L. (1979). *J. Mol. Biol.* In preparation.

STUART, D. I., LEVINE, M., MUIRHEAD, H. & STAMMERS, D. K. (1979). *J. Mol. Biol.* In the press.